THE MECHANICS OF PLGA NANOFIBER SCAFFOLDS WITH BIOMIMETIC GRADIENTS IN MINERAL FOR TENDON ENTHESIS REPAIR

- SUPPLEMENTAL DOCUMENT -

Lipner J[1,2]
Liu W[4]
Liu Y[3]
Boyle J[1,2]
Genin GM[3]
Xia Y[5]*
Thomopoulos S[1,2,3]*

Washington University in St. Louis, St. Louis, Missouri:
[1]Department of Biomedical Engineering
[2]Department of Orthopaedic Surgery
[3]Department of Mechanical Engineering and Materials Science

Georgia Institute of Technology, Atlanta, GA:
[4]Department of Chemical and Biomolecular Engineering
[5]The Wallace H. Coulter Department of Biomedical Engineering

***Corresponding Authors:**

Biomechanics: Stavros Thomopoulos, Ph.D.
Washington University
Department of Orthopaedic Surgery
660 South Euclid, Campus Box 8233
St. Louis, MO 63110
Phone: 314-362-8605
Fax: 314-362-0334
Email: ThomopoulosS@wudosis.wustl.edu

Scaffold synthesis: Younan Xia, Ph.D.
Department of Biomedical Engineering
Georgia Institute of Technology
901 Atlantic Dr NW
Atlanta, GA 30332
Phone: (404) 385-3209
Fax: (404) 385-7493
E-mail: younan.xia@biomed.gatech.edu

A. Estimation of mineral volume fraction from energy dispersive x-ray (EDX) measurements

Mineral volume fractions were estimated from energy dispersive x-ray (EDX) measurements through the following four steps:

1. **Correction for undercounting of C atoms.** A series of samples were analyzed using both EDX and mass spectroscopy to estimate the relative numbers of C and Ca atoms per unit volume. As expected, EDX undercounted the C atoms relative to the more accurate mass spectroscopy estimates. An approximately linear correction was found for the ratio of Ca atoms to the combined number of C and Ca atoms. We term the as-measured ratio "EDX" and the adjusted ratio "$EDX_{adjusted}$."
2. **Estimation of fiber-level mass fractions from adjusted EDX measurements.** The relative numbers of C and Ca atoms per unit volume were converted to fiber-level mass fractions based upon the composition of the scaffold (Tables S1-S3).
3. **Estimation of fiber-level volume fractions from fiber-level mass fractions.** Mass fractions were converted to fiber volume fractions using estimates of density from the literature.
4. **Estimation of scaffold-level volume fractions from fiber-level volume fractions.** Scaffold-level volume fractions were scaled down from estimated fiber-level volume fractions based upon measurements of polymer volume fraction in the scaffolds.

Table S1: Molar masses used in computations.

Element	**Molar mass**
Calcium	40.08 g/mol
Carbon	12.01 g/mol
Hydrogen	1.008 g/mol
Phosphorus	30.97 g/mol
Oxygen	15.999 g/mol

Table S2: Calculation of hydroxylapatite composition.

Formula, including substitutions	$\boldsymbol{Ca_{10-x}(PO_4)_{6-x}(CO_3)_{x+y}(OH)_{2-x-2y}}$
Formula assuming bone-like carbonation of 1.1wt%, and 85:15 ratio between A and B type substitutions, which leads to x = 0.154 and y = 0.027 (1)	$\boldsymbol{Ca_{9.85}(PO_4)_{5.85}(CO_3)_{0.182}(OH)_{1.79}}$
Total Molecular Weight	991.128 g/mol
Calcium Mass	394.61 g/mol
Calcium Mass Fraction	0.398
Carbon Mass	2.2 g/mol
Carbon Mass Fraction	0.002
Density	3.16 g/ml

Table S3: Calculation of poly(lactic-co-glycolic acid) (PLGA) (85:15) composition.

Glycolic Acid formula	$\boldsymbol{C_3H_6O_3}$
Molecular Weight	90.08 g/mol
Lactic Acid formula	$\boldsymbol{C_2H_4O_3}$
Molecular Weight	76.05 g/mol
85:15 PLGA formula	$\boldsymbol{C_{2.85}H_{5.7}O_3}$
Molecular Weight	87.99 g/mol
Density	1.27 g/ml
Calcium Mass Fraction	0.0
Carbon Mass Fraction	0.39

A.1 Correction for undercounting of C atoms.

EDX yielded estimates of relative numbers of atoms per unit volume:

$$EDX = \left(\frac{N_{Ca}}{N_{Ca}+N_C}\right) \quad (1)$$

where N_{Ca} and N_C are estimates of the number Ca and C atoms per unit volume, respectively. However, this estimate was high compared to those obtained using inductively coupled plasma mass spectroscopy (ICPMS) (Figure S1). ICPMS is considered to be more accurate that EDX due to an inherent weakness of EDX in detecting C. EDX estimates were therefore adjusted to fitting ICPMS data. Since the two measurements must agree at their limits (i.e., at ratios of zero and one) and the data lie below a linear slope of 1, we expect that the relationship between EDX and ICPMS estimates to be concave up (Figure S1). We assumed a linear error in the ratio $X = N_C/N_{Ca}$, and fitted the data to find a correction factor α, where $X_{adjusted} = \alpha X$. Rearranging, the adjusted EDX measurement was:

$$EDX_{adjusted} = \frac{EDX}{EDX + \alpha(1 - EDX)} \quad (2)$$

Note that this predicts a concave up relationship of $EDX_{adjusted}$ versus EDX, while the data plotted in Figure S1 appear to show a concave down trend. However, the error bars on the data (not shown) are sufficiently large to admit either interpretation. Additionally, the linear fit $EDX_{adjusted} = 0.476EDX$ is reasonable over the range shown (R^2 = 0.82). Fitting the model of equation (2) to these same data yields an estimate of α =2.7.

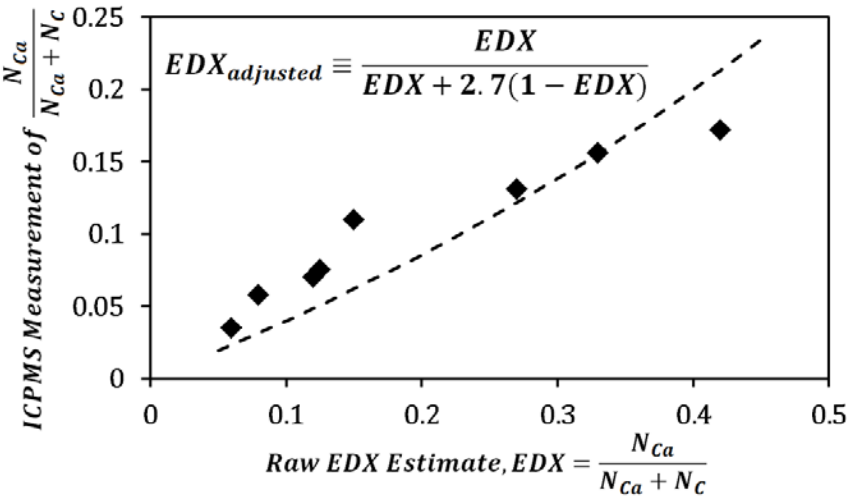

Figure S1: A fit to the relationship between EDX and ICPMS measurements made on identical specimens was used to correct raw EDX estimates of atomic fraction.

A.2 Estimation of mass fractions from adjusted EDX measurements.
The atomic fraction was converted to a mass fraction using the atomic masses of Ca and C:

$$EDX_{adjusted} = \frac{N_{Ca}}{N_{Ca} + N_C^{adjusted}} = \frac{P_{Ca}}{P_{Ca} + \left(\frac{40.08}{12.01}\right) P_C^{adjusted}} \tag{3}$$

where P_{Ca} and $P_C^{adjusted}$ are scaffold-level mass densities of Ca and C, respectively, and (40.08/12.01) is the ratio of molar masses of Ca and C. These in turn were converted to scaffold-level mass densities P_{HA} of hydroxylapatite and P_{PLGA} of PLGA. Since Ca comprises 39.8% of the mass of hydroxylapatite, $P_{HA} = P_{Ca}/0.398 = 2.51 P_{Ca}$ was used. Since C comprises 0.2% of hydroxylapatite and 39.0% of PLGA, the PLGA volume fraction was estimated from $P_C^{adjusted} = 0.002 P_{HA} + 0.390 P_{PLGA}$, or $P_{PLGA} = 2.56 P_C^{adjusted} - 0.0129 P_{Ca}$. Thus,

$$EDX_{adjusted} = \frac{0.398 P_{HA}}{0.398 P_{HA} + \left(\frac{40.08}{12.01}\right)(0.002 P_{HA} + 0.390 P_{PLGA})} = \frac{1}{1.02 + 3.27 P_{PLGA}/P_{HA}} \tag{4}$$

or:

$$\frac{P_{HA}}{P_{PLGA}} = \frac{3.27}{\left(\frac{1}{EDX_{adjusted}} - 1.02\right)} \tag{5}$$

A.3 Estimation of fiber-level volume fractions from fiber-level mass fractions
The ratio of scaffold-level volume fractions of hydroxylapatite and PLGA, φ_{HA} and φ_{PLGA}, were then estimated using the mass densities of hydroxylapatite and PLGA, which were taken as ρ_{HA}=3.16 g/cm^3 and ρ_{PLGA}=1.27 g/cm^3, respectively:

$$\frac{\varphi_{HA}}{\varphi_{PLGA}} = \frac{P_{HA}}{P_{PLGA}} \frac{\rho_{PLGA}}{\rho_{HA}} \tag{6}$$

A.4 Estimation of scaffold-level volume fractions from fiber-level volume fractions

Combining,

$$\varphi_{HA} = \frac{3.27}{\left(\frac{1}{EDX_{adjusted}} - 1.02\right)} \frac{\rho_{PLGA}}{\rho_{HA}} \; \varphi_{PLGA} = \frac{1.31}{\left(\frac{1}{EDX_{adjusted}} - 1.02\right)} \; \varphi_{PLGA} \tag{7}$$

Finally, from Equation (2), and noting that $\alpha > 1$ and that neither φ_{PLGA} nor α are known to within more than two significant figures,

$$\varphi_{HA} \approx \frac{1.3EDX}{\alpha(1 - EDX)} \; \varphi_{PLGA} \tag{8}$$

Equation (8) was used in all subsequent analyses to convert the relative atomic fraction measurement from EDX to a scaffold-level volume fraction of hydroxylapatite. Noting that in our scaffolds $\varphi_{PLGA} \approx 0.13$ and substituting for α, $\varphi_{HA} \approx 0.063EDX/(1 - EDX)$.

B. Parallel and series estimates, and Hashin-Shtrikman Bounds

B.1 Parallel Estimate

The parallel estimate was made by assuming that fibers of mineral were synthesized in parallel with fibers of PLGA, and that all of these were aligned with the direction of loading.

$$E_{composite} = E_{PLGA}\varphi_{PLGA} + E_{HA}\varphi_{HA} + E_{VOIDS}\varphi_{VOIDS} \tag{9}$$

Where E is a modulus and φ is a scaffold-level volume fraction, the subscript text refers to three components of the composite (PLGA, mineral (HA), and voids), and E_{VOIDs}=0. Note that, as discussed by Hill (1964), this approximation neglects the additional stiffening that could occur because of Poisson mismatch in the case of a mineral sheath adherent to the PLGA fibers, and hence is not a true upper bound (2). However, this estimate is sufficiently stiff to serve as a guideline for comparing our data to the greatest stiffening possible.

B.2 Series Estimate

The most naïve series estimate one could choose would be that in which PLGA, HA, and air are stacked atop one another, yielding the following estimate of the composite stiffness:

$$E_{composite} = \frac{1}{\frac{\varphi_{PLGA}}{E_{PLGA}} + \frac{\varphi_{HA}}{E_{HA}} + \frac{\varphi_{AIR}}{E_{AIR}}} \tag{10}$$

This leads to an estimate of 0 as a modulus. However, this estimate must obviously be rejected because it fails to account for the observation that no reasonable mineralized PLGA scaffold would be tested or grafted into a surgical repair with a layer of air on one end. Therefore, the correct composite bound to use as a guideline is based upon a series combination of mineral and PLGA on a fiber:

$$E_{fiber} = \frac{\varphi_{PLGA} + \varphi_{HA}}{\frac{\varphi_{PLGA}}{E_{PLGA}} + \frac{\varphi_{HA}}{E_{HA}}} \tag{11}$$

This must then be scaled downwards to account for the air:

$$E_{composite} = (\varphi_{PLGA} + \varphi_{HA})E_{fiber} = \frac{(\varphi_{PLGA} + \varphi_{HA})^2}{\frac{\varphi_{PLGA}}{E_{PLGA}} + \frac{\varphi_{HA}}{E_{HA}}} \tag{12}$$

As mentioned in the discussion, this is not a true lower bound because, as occurs with the 10SBF scaffolds, it is possible for mineral to be added to the composite that does not connect at all to PLGA. However it serves as a guideline to determine whether a mineralization pattern is effective at stiffening a fibrous scaffold.

B.3 Hashin-Shtrikman Bounds

The Hashin-Shtrikman bounds are the best estimates available for the stiffness of a composite containing random dispersions of a reinforcing phase, in the absence of any information about the structures of and interactions amongst these phases. The equations are reproduced here, along with our application of them to account for the fibrous nature of the PLGA phase in the scaffolds of interest.

The model used was a three-phase composite of PLGA, voids, and mineral. The PLGA and mineral were idealized as mixing into homogeneous fibers that contained no voids. The scaffold-level PLGA volume fraction was set to $\varphi_{PLGA} = 0.13$, and the scaffold-level mineral volume fraction was allowed to vary over the range $0 \leq \varphi_{HA} \leq 0.87$. The fibers grew in diameter as mineral was added. These fibers had a scaffold-level volume fraction of $\varphi_{PLGA}+\varphi_{HA}$, with voids of volume fraction $\varphi_{voids} = 1 - \varphi_{PLGA} - \varphi_{HA}$ filling the remaining space. The fiber-level volume fractions of PLGA and mineral within fibers were:

$$f_{PLGA} = \frac{\varphi_{PLGA}}{\varphi_{PLGA} + \varphi_{HA}} \tag{13}$$

$$f_{HA} = \frac{\varphi_{HA}}{\varphi_{PLGA} + \varphi_{HA}} \tag{14}$$

Bounds were studied for the effective bulk and shear moduli, K_e^{fiber} and G_e^{fiber}, respectively, of a fiber containing a volume fraction f_{PLGA} of PLGA and a volume fraction $f_{HA} = 1 - f_{PLGA}$ of hydroxylapatite. The Hashin-Shtrikman lower bound K_L^{fiber} and upper bound K_U^{fiber} for K_e^{fiber} are (3):

$$K_e^{fiber} \geq K_L^{fiber} = K_{PLGA} + \frac{(1 - f_{PLGA})}{\frac{1}{(K_{HA} - K_{PLGA})} + \frac{3f_{PLGA}}{(3K_{PLGA} + 4G_{PLGA})}} \tag{15}$$

and

$$K_e^{fiber} \leq K_U^{fiber} = K_{HA} + \frac{(1 - f_{HA})}{\frac{1}{(K_{PLGA} - K_{HA})} + \frac{3f_{HA}}{(3K_{HA} + 4G_{HA})}} \tag{16}$$

where G_{PLGA} and K_{PLGA} are the shear and bulk moduli of PLGA, and G_{HA} and K_{HA} are the shear and bulk moduli of hydroxylapatite. The Hashin-Shtrikman lower bound G_L^{fiber} and upper bound G_U^{fiber} for G_e^{fiber} are (3):

$$G_e^{fiber} \geq G_L^{fiber} = G_{PLGA} + \frac{(1 - f_{PLGA})}{\frac{1}{(G_{HA} - G_{PLGA})} + \frac{6f_{PLGA}(K_{PLGA} + 2G_{PLGA})}{5(3K_{PLGA} + 4G_{PLGA})}} \quad (17)$$

and

$$G_e^{fiber} \leq G_U^{fiber} = G_{HA} + \frac{1 - f_{HA}}{\frac{1}{(G_{PLGA} - G_{HA})} + \frac{6f_{HA}(K_{HA} + 2G_{HA})}{5(3K_{HA} + 4G_{HA})}} \quad (18)$$

The elastic modulus of the fibers could then be bounded by:

$$\frac{9K_L^{fiber}G_L^{fiber}}{3K_L^{fiber} + G_L^{fiber}} \leq E_e^{fiber} \leq \frac{9K_U^{fiber}G_U^{fiber}}{3K_U^{fiber} + G_U^{fiber}} \quad (19)$$

The scaffold-level bounds were obtained by scaling the bounds on fiber-level moduli by the scaffold-level fiber volume fraction, $\varphi_{PLGA}+\varphi_{HA}$:

$$E_e^{scaffold} = (\varphi_{PLGA} + \varphi_{HA})E_e^{fiber} \quad (20)$$

C. References

1. Pasteris JD, Yoder CH, Sternlieb MP, Liu S. Effect of carbonate incorporation on the hydroxyl content of hydroxylapatite. Mineralogical Magazine.76:2741-59. 2012.

2. Hill R. Theory of mechanical properties of fibre-strengthened materials: I. Elastic behaviour. Journal of the Mechanics and Physics of Solids.12:199-212. 1964.

3. Hashin Z, Shtrikman S. Note on a variational approach to the theory of composite elastic materials. Journal of the Franklin Institute.271:336-41. 1961.